Environmental Science and Pollution Research (2023) 30:106982–106995
https://doi.org/10.1007/s11356-022-24064-8

ENVIRONMENTAL IMPACTS AND CONSEQUENCES OF URBAN SPRAWL

Effective removal of Cr (VI) ions using low-cost biomass leaves (*Sambucus nigra* L.) in aqueous solution

Humberto Bonilla Mancilla[1] · Mauro Rodríguez Cerrón[1] · Percy Grijalva Aroni[1] · Jesús Eduardo Pomachagua Paucar[1] · Candelaria Tejada Tovar[2] · Manoj Kumar Jindal[3,4] · Ganesan Gowrisankar[4,5]

Received: 22 July 2022 / Accepted: 2 November 2022 / Published online: 9 November 2022

Abstract

The tannery industries have become an important part of societal growth; however, these processes have produced huge volumes of effluents containing heavy metals, particularly Cr(VI) oxyanions. The study is crucial and cost-effective for reducing the chromium (VI) from industrial wastewater. In order to meet the sustainable development goal (SDG) objective 6.3, the capacity of *Sambucus nigra* L. to adsorb heavy metal is established with the purpose of eradicating hazardous chemical contamination and reducing pollution. In this study, discontinuous tests were carried out to determine the efficiency of Cr(VI) sorption on leaves of *Sambucus nigra* L. Adsorption factors such as pH, temperature, adsorbent dosage, and contact time were evaluated. At a dosage of 3 g/L and pH 2, an efficiency of 98.22% was achieved under favorable conditions. The equilibrium and kinetic models that best fitted the experimental data are non-linear Freundlich and; pseudo-second order, and intra-particle diffusion, respectively. The thermodynamic parameters of the adsorption process, including Gibbs free energy (ΔG^0), enthalpy (ΔH^0), and entropy (ΔS^0), were measured at 291, 303, 323, and 343 K, indicating that the phenomena was spontaneous and endothermic. The chemical analyses and surface morphology of the adsorbent were analyzed using SEM (scanning electron microscopy), EDS (energy dispersive spectroscopy), FTIR (Fourier transform infra-red), XRD (X-ray diffraction), and ICP-OES (inductively coupled plasma optical-emission spectroscopy) techniques. The results showed that *Sambucus nigra* L. has a significant removal efficiency of Cr(VI) in the contaminated solutions, establishing adsorbent as a low cost, readily available, and environmentally friendly and ensuring its potential for industrial usage.
Graphical abstarct.

Keywords *Sambucus nigra* L. · Adsorption of chromium · Heavy metal

Responsible Editor: Tito Roberto Cadaval Jr

✉ Humberto Bonilla Mancilla
hbonilla@uncp.edu.pe

✉ Manoj Kumar Jindal
manojjindal1989@gmail.com

Mauro Rodríguez Cerrón
m1rodriguez@uncp.edu.pe

Percy Grijalva Aroni
plgrijalva@uncp.edu.pe

Jesús Eduardo Pomachagua Paucar
jpomachagua@uncp.edu.pe

Candelaria Tejada Tovar
ctejadat@unicartagena.com

Ganesan Gowrisankar
geogowri30@gmail.com

[1] Faculty of Forestry and Environmental Sciences, National University of the Center of Peru, Huancayo, Peru

[2] Department of Chemical Engineering, University of Cartagena, Cartagena, Colombia

[3] Department of Chemistry, Indian Institute of Technology, Bhilai, India

[4] Present Address: Divecha Centre for Climate Change, Indian Institute of Science, Bangalore, India

[5] Department of Geology, Anna University, Chennai, Tamil Nadu, India

Introduction

Currently, industrial wastewater management is unsustainable, which has a detrimental impact on achieving sustainable development by 2030. The presence of metal ions and organic compounds in water supplies is a result of economic expansion and development (Mughal et al. 2022). Biological molecules, unlike metal ions, are mostly susceptible to organic reduction (Beksissa et al. 2021). Because of their high toxicity and bioavailability, metal ions are a constant source of worry in various ecosystems. In this sense, chromium metal is found in many ecosystems because of a lack of strategic management in corporate social responsibility (CSR) (Peng et al. 2020). Metallurgical industries, mining, tanneries, paints, batteries, radiators, smelters, and mineral weathering all emit considerable quantities of chromium (Rouhaninezhad et al. 2020; Thabede et al. 2020; Tao et al. 2021). Chromium's most prevalent oxidation states in the environment are Cr (III) and Cr (VI). Among them, Cr (III) is essential for cellular metabolism (sugars, fats, and proteins) in humans, animals, and plants (Cherdchoo et al. 2019). Soil (humic acid, pH, redox potential) and groundwater oxidize Cr (III), transforming it to Cr (VI) metallic element. Even in trace concentration, this metallic state is more harmful and toxic to public health because of its teratogenic, carcinogenic, and mutagenic properties (Cherdchoo et al. 2019; Shooto 2020b; Khalil et al. 2021).

According to the EPA (Environmental Protection Agency), the maximum allowed contamination level of water standard for total chromium is 0.1 mg/L (US EPA 2022). However, the WHO (World Health Organization) standard recommends 0.05 mg/L (WHO 2020; WHO, n.d.). In view of these negative effects and to improve public health, Cr (VI) ions must be removed prior to discharge. To date, technologies such as coagulation, filtration, chemical precipitation, reverse osmosis, ion exchange, and membrane systems have been used (Ray et al. 2020; Rouhaninezhad et al. 2020; Tejada et al. 2021). However, these technologies have certain drawbacks, such as high operating costs, generation of secondary pollution, and limited efficiency. In this sense, adsorption technology is considered a more efficient and easier to monitor (Cherdchoo et al. 2019), low cost, and environmentally friendly way (Shooto 2020b). Many adsorbents have been investigated for managing the Cr (VI) from industrial effluents, including coffee and tea residues (Cherdchoo et al. 2019), tea residues (Nigam et al. 2019), black cumin seed (Thabede et al. 2020), *Harpagophytum* residues (Shooto 2020b), *Eichhornia crassipes* and *Lemna minor* leaves (Balasubramanian et al. 2020), mango bark (Pathania et al. 2020), *Mentha piperita* residues (Al et al. 2020), *Acacia* sawdust (Khalid et al. 2018), rice husk (Khalil et al. 2021), and water hyacinth residues (Kumar and Chauhan 2019). In this line, it is always interesting to search for new adsorbents that are affordable, accessible, effective, and easy to apply.

Sambucus nigra L., sometimes referred to as "Sauco," is a member of the Caprifoliaceae family and is indigenous to Asia, Europe, and America (Ağalar 2019; Domínguez et al. 2020; Ruíz and Mejía 2020). It is a plant well-known for its physical, chemical, and biological properties. It is a tree or shrub that ranges in height from 1 to 12 m which has longitudinal fractures, deep furrows, and aged shafts. It has leaves with seven to nine leaflets that are imparipinnate, oblong, and pointed at the apex and have serrated edges that are 4 to 6 cm long and 3 to 7 cm wide (National Institute for the Defense of Competition and the Protection of Intellectual Property 2018; Ağalar 2019; Quiñones et al. 2020; Navas et al. 2021; Boroduske et al. 2021). The tree has been demonstrated to have antiviral qualities, which have been used to treat COVID-19 (Boroduske et al. 2021; Huaccho et al. 2020), as antioxidants to treat malignant cells (Filip et al. 2021), and for the food sector (Ağalar 2019). These goodnesses are due to chemical components such as polyphenols, phenolic acids, flavonoids, and tannins (Filip et al. 2021). In addition to these chemical elements, *Sambucus nigra* L. contains 41.9% fiber, 21.2% protein, 18.3% dry matter, and 19.4% carbohydrates (Quiñones et al. 2020); likewise, chemical components such as polysaccharides (cellulose, hemicellulose, and lignin), these chemical groups characterize the biomaterial as a best option for the treatment of heavy metals from industrial effluents (Kumar and Chauhan 2019).

Sambucus nigra L. has not yet been studied for its potential to adsorb heavy metals. Therefore, based on the aforementioned criteria, the biomass leaves were employed as an adsorbent to control the chromium (VI) from synthetic solutions. FTIR, SEM, and X-ray diffraction analyses were performed to know the surface characteristics and determine the chromium (VI) adsorption, and the adsorption experiments were carried out batch-wise and it was studied based on evaluating the effect of contact time, adsorbent dosage, pH of the sample, and adsorption capacity in aqueous solution.

Materials and methods

Materials and reagents

The chemical reagent used for the execution of the research was highly pure and analytical grade. Potassium dichromate ($K_2Cr_2O_7$) of 99.0% purity, purchased from Spectrum

Chemical Mfg. Corp. All the glass materials were rinsed with double distilled water and dried in an oven at 55 °C before use.

Preparation of the bioadsorbent

Four kilograms of *Sambucus nigra* L. leaves was collected from the university campus of the Universidad Nacional del Centro del Perú, washed with tap water to remove dust and other adhered particles, and then rinsed with double distilled water. They were then dried at 65 °C for 72 h until they reached a constant weight, ground, and sieved with mesh No. 60 (ASTM), labeled, and stored in drying conditions until further use.

Batch adsorption studies

A standard chromium stock solution of 1000 mg/L was made by dissolving the required amount of potassium dichromate in double distilled water. Working solutions at different concentrations were made by successive dilutions of the standard solution. Adsorption experiments were performed in 50 mL of 10 mg/L chromium (VI) solution at a dose of 3 g/L of adsorbent. The pH of the solution was adjusted by adding a few drops of 0.1 N HNO_3 or 0.1 N NaOH. After the contact process, they were filtered with Whatman N° 41 filter paper. The residual Cr (VI) concentration was analyzed using the ANALYTIK JENA NOVA PRO-400 atomic absorption spectrophotometer. Sorption tests were conducted at various Cr (VI) concentrations, pH levels, temperatures, reaction times, and adsorbent dosages. The adsorption capacity of *Sambucus nigra* L., q_e (mg/g), was determined using the mass balance equation as presented in Eq. 1.

$$q_e = \frac{(C_o - C_e)}{m} * V \tag{1}$$

where C_o (mg/L) and C_e (mg/L) represent the initial and equilibrium concentration of Cr (VI) respectively, V is the volume of the solution (L), and m is the weight of the dry biomass (g).

The percentage removal capacity of Cr (VI) was calculated by using the Eq. 2:

$$\%R = \frac{C_o - C_f}{C_o} x100 \tag{2}$$

where C_o and C_f (mg/L) are the initial and final Cr (VI) concentration before and after adsorption, respectively. The maximum adsorption capacity and the efficiency of the sorbate-biosorbent phenomenon were determined in relation to the experimental adsorption data.

Equilibrium study

To determine the sorbent-sorbate ratio at different Cr (VI) concentrations and equilibrium data, adsorption isotherms were modeled. In this study, Langmuir and Freundlich equilibrium isotherms were used.

Langmuir isotherm model

The Langmuir isotherm (Langmuir 1918) suggests that the phenomenon occurs on a homogeneous surface forming a monolayer when the adsorbent has reached saturation (each active site was occupied by one element), with no interaction between the adsorbed metals, uniform energy, and no transmission of the adsorbate (Ighalo and Adeniyi 2020).

The linearized Langmuir equation is presented in Eq. 3.

$$\frac{C_e}{q_e} = \frac{1}{K_L q_m} + \frac{C_e}{q_m} \tag{3}$$

where q_m (mg/g) is the maximum adsorption capacity by the adsorbent on the monolayer and K_L (L/mg) is the energy constant of the adsorption process. The values of q_m and K_L (Langmuir constant) were determined from the slope and the interaction of the C_e/q_e vs C_e figure. Also, the feasibility of the adsorption process was determined by the dimensionless factor (R_L). The R_L values were determined based on the Eq. 4:

$$R_L = \frac{1}{1 + K_L C_o} \tag{4}$$

The R_L values represents whether the adsorption is unfavorable or favorable. Unfavorable when $R_L > 1$, linear when $R_L = 1$, favorable when it is between $0 < R_L < 1$ and irreversible when $R_L = 0$.

Non-linear Langmuir equation is shown in Eq. 5.

$$q_e = \frac{q_m K_L C_e}{1 + K_L C_e} \tag{5}$$

The Freundlich isotherm

This model proposes a multilayer sorption with interactions between the adsorbed particles and heterogeneous energy distribution at the active sites, i.e., the binding forces between the sorbent-sorbate are stronger at the beginning of the process and decreases as the level of accumulation increases. The linearized form of the Freundlich isotherm (Freundlich 1906) is shown in Eq. 6. The non-linear equation is presented in Eq. 7.

$$Logq_e = LogK_F + \frac{1}{n}LogC_e \tag{6}$$

$$q_e = K_F C_e^{\frac{1}{n}} \tag{7}$$

where q_e is the amount of contaminant removed (mg/g), K_F (mg/g) is the Freundlich's constant, C_e is the equilibrium concentration (mg/L), and n is related to adsorption capacity and adsorption intensity. The values of K_F and n are determined from the slope and intercept of the linear figure Log q_e vs Log C_e.

Study of the kinetics

The main factors in the adsorption process are mass transfer, chemical reaction, and reaction rate (Ighalo and Adeniyi 2020; Tejada et al. 2021). The mass transfer kinetics is described by the velocity between the aqueous and solid phase (Bazzazzadeh et al. 2020). To calculate the removal rate, the following times were considered: 2, 4, 15, 25, 35, 55, 100, 130, and 150 min with a concentration of 10 mg/L.

Pseudo-first-order model

The model refers that the mass transfer of the adsorbate ions is corresponding to the active sites on the adsorbate surface could due to carbonyl group, alcohol, carboxylic acid, or phenols, N–H bend of amine with an unsaturated hydrocarbon, alkyl halides. The linearized form of the pseudo-first-order equations is presented in Eq. 8.

$$Log\left(q_t - q_e\right) = -\frac{K_1}{2.303}t + Logq_e \tag{8}$$

where q_t and q_e (mg/g) are the amount of Cr (VI) adsorbed at time t (min) and equilibrium, respectively and first-order rate constant is represented by K_1 (min^{-1}). The value of q_e and K_1 was determined from the intercept and slope of the log $(q_e - q_t)$ vs t plot. The non-linear form of pseudo-first-order equation is shown in Eq. 9.

$$q_t = q_e\left[1 - \exp(-k_1 t)\right] \tag{9}$$

Pseudo-second-order model

To determine the adsorbate contact time at the solid–liquid interface, adsorption mechanism depending on the physical and chemical characteristics of the adsorbent, crucial factors in the construction of wastewater treatment facilities. Furthermore, this model characterizes all the processes of adsorption, such as internal-exterior particle diffusion, and describes the chemical processes involving valence forces via electron exchange between adsorbent and adsorbate. The linearized equation of the model is shown in Eq. 10.

$$\frac{t}{q_t} = \frac{t}{q_e} + \frac{1}{K_2 q_e^2} \tag{10}$$

where K_2 is the second-order rate constant (mg/g min). The value of K_2 and q_e were estimated from the intercept and slope of the t/q_t vs t figure. The non-linear form of pseudo-second-order equation is presented in Eq. 11.

$$q_t = \frac{q_e^2 K_2 t}{1 + q_e K_2 t} \tag{11}$$

The kinetic of adsorption process was also evaluated by the Webber's pore-diffusion equation which is shown in Eq. 12.

$$q_t = K_{int} t^{\frac{1}{2}} + C \tag{12}$$

where K_{int} is the rate constant for the intraparticle diffusion rate.

Thermodynamic studies

Thermodynamic parameters determine the nature of the adsorption procedure (Nigam et al. 2019). For the thermodynamic analysis of the sorption process, the Gibbs free energy change (ΔG°), entropy change (ΔS°), and enthalpy change (ΔH°) were determined in relation to temperatures 291, 303, 323, and 343 K. The calculation of the thermodynamic parameters using the adsorption equilibrium constant and K_d is presented in Van't Hoff Eqs. 13 and 14. K_d dimensionless equation explained by Lima et al. (2019) is considered as shown in Eq. 15.

$$\Delta G^o = \Delta H^o - T\Delta S^o \tag{13}$$

$$LnK_d = \frac{\Delta S^o}{R} - \frac{\Delta H^o}{RT} \tag{14}$$

$$K_d = \frac{q_e}{C_e} \times \frac{m}{V} \tag{15}$$

where ΔG° is the Gibbs free energy (kJ/mol), ΔH° is the sorption enthalpy variation (kJ/mol), T is the temperature (K), ΔS° is the entropy (kJ/mol K), R is the gas constant (8.314 J/mol K), m is the mass of the adsorbent, and V is the volume of the adsorbate solution.

Results and discussions

The effectiveness of adsorption processes of experimental batch technique is determined by using the several factors (pH, adsorbent dosage, contact duration).

Effect of pH

The pH point of zero charge (pHpzc) of the adsorbent is a very important factor in the sorption process, which is defined as the pH value of the aqueous solution at which the net surface charge of the sorbent is neutral or null (Labied et al. 2018) and was determined following the experimental protocol defined by Lavado-Meza et al. (2021), for which a series of solutions was prepared with 0.05 g of adsorbent in 50 ml of deionized water, initial pH levels from 2.0 to 12.0, pH were adjusted using 0.1 M solutions of HCl and NaOH, and samples were shaken at 150 rpm at 20 °C for 24 h. The final pH levels were then measured and the final pH values (pH_f) were plotted against the initial pH values (pH_i). The pHpzc of the adsorbent was 5.86, which is shown in Fig. 1. This implies that at pH values lower than pHpzc the adsorbent acquired positive charges determining a higher performance in the removal of Cr (VI) anions, likewise, at pH > pHpzc, the adsorbent acquired negative charges significantly reducing the removal of Cr (VI) ions. This is due to strong electrostatic attraction between the positively charged surface of the adsorbent and the dichromate ($Cr_2O_7^{2-}$) and chromate ($HCrO_4^-$) anion species (in acidic medium, anion $HCrO_4^-$ is the more dominant) of the adsorbate, resulting in increased adsorption efficiency. These results are similar to those obtained by Baruffi et al. (2019) and Haroon et al. (2020).

Figure 2 shows the adsorption capabilities of *Sambucus nigra* L. adsorbent to adsorb Cr (VI) at various pH levels (range of 2 to 12) with chromium species distribution as described by Shen and Ke (1986) and Spessato et al. (2021). During the removal process, pH becomes a crucial parameter for determining adsorption effectiveness. The maximum

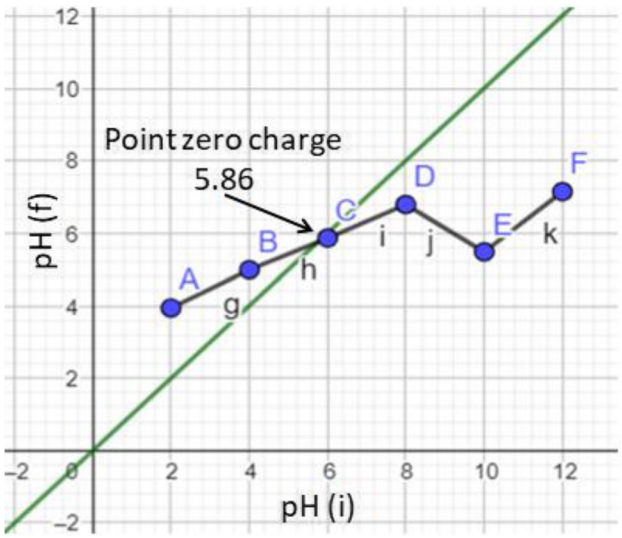

Fig. 1 pH point of zero charge (pHpzc) graph

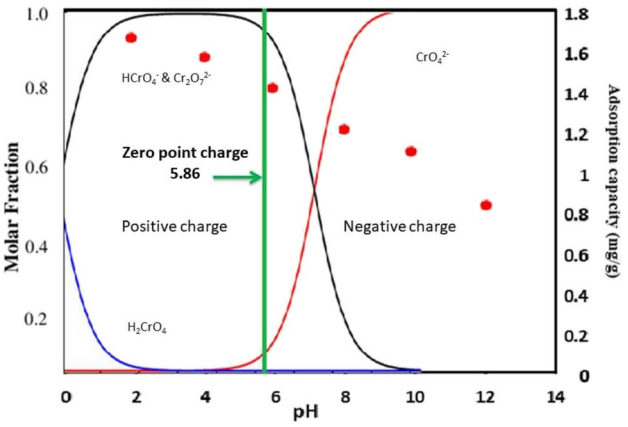

Fig. 2 Effect of pH on Cr (VI) adsorption with Cr species distribution

removal efficiency was achieved at pH = 2.0 (98.2%) with a q_e of 1.64 mg/g, while the minimum efficiency at pH = 12 was 49.8% with a q_e of 0.83 mg/g.

At different pH levels, Cr (VI) appears to take on distinct ionic forms. Cr (VI) occurs mostly in the form of $HCrO_4^-$, and $Cr_2O_7^{2-}$ in the pH range 2.0 to 6.0, with $HCrO_4^-$ dominating (Ghorbani et al. 2020; Pathania et al. 2020). The maximum removal was determined due to electrostatic attraction at acidic pH between $HCrO_4^-$ ions and the adsorbent surface (protonated H+) with positive charge (below the zero charge point 5.86), which leads to an increase in the amount adsorbed; however, a decrease in removal was observed at pH 6.0 to 12, which could be due to negative charge on adsorbent surface, resulting in a reduction of the adsorbed amount. According to Saha and Orvig (2010), there are four mechanisms for removing chromium from aqueous solution: (1) anionic adsorption, (2) reduction coupled to adsorption, (3) cationic and anionic adsorption, and (4) reduction and anionic adsorption. Consequently, the Cr (VI) adsorption ions could be referred to as mechanism 4 (reduction and anionic adsorption). A fraction of Cr (VI) would be reduced to Cr (III) by the action of the functional groups on the surface of the biomaterial and dissolving in the solution, while the majority of Cr (VI) ions would be adsorbed by the adsorbent via electrostatic attraction (Ghorbani et al. 2020; Pathania et al. 2020; Shooto 2020b).

Effect of adsorbent dose

The adsorption capacity of the adsorbent at a defined initial concentration depends on the dose of the biomaterial. The present study employed an initial concentration of 5 mg/L Cr (VI), a contact time of 25 min, and a pH of 2 to investigate the effect of adsorbent dose ranging from 1 to 5 g/L.

As demonstrated in Fig. 3, increasing the adsorbent dosage from 1 to 3 g/L increased the adsorption percentage from

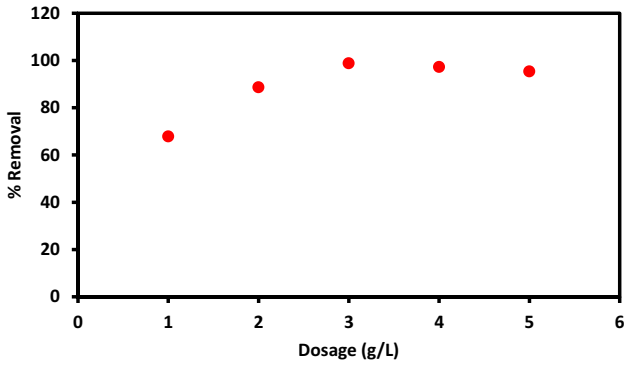

Fig. 3 Effect of adsorbent dosage (g/L) on adsorption of Cr (VI)

67.86 to 98.78. Indeed, this rise reflects an increase in the number of active groups (carbonyl group, alcohol, carboxylic acid, or phenols, N–H bend of amine with an unsaturated hydrocarbon, alkyl halides) as well as an expansion of contact surface areas. In addition, at doses ranging from 4 to 5 g/L, chromium (VI) adsorption was reduced from 97.24 to 95.34%. This occurrence was presumably caused by adsorption site overlapping, an imbalance in sorbate-adsorbent concentration, and overcrowding of biosorbent particles in the solution (Al et al. 2020; Bazzazzadeh et al. 2020). According to Khalil et al. (2020), the low removal rate of Cr (VI) with increasing adsorbent dose could be due to unsaturated binding sites, which shows that the adsorption sites increase with increasing adsorbent dose, but the ratio between the doses determined with the initial ratio of Chromium (VI) ions adsorption is reduced.

Effect of contact time

The percentages of Cr (VI) removal capacity as a function of time are shown in Fig. 4. In an aqueous solution at a concentration of 15 mg/L, pH = 2, 3 g/L adsorbent, and 18 °C, the impact of contact time (2–150 min) was studied.

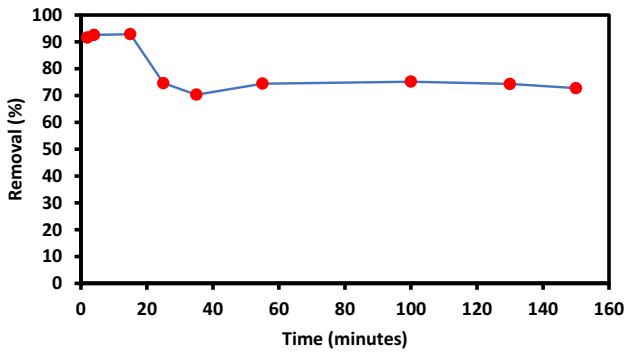

Fig. 4 Effect of contact time on adsorption of Cr (VI) via *Sambucus nigra* L

The removal capacity of Cr (VI) by the adsorbent *Sambucus nigra* L. was very fast in the initial phase, achieving a removal of 92.83% in the first 15 min, but this effect gradually decreased with time, most likely due to competition between the reduction of surface active sites and Cr (VI) ions, so that after 35 min, 70.31% was removed. At the beginning of the sorption process, the percentage of chromium removal was higher due to a higher availability of the surface area and the porosity of the adsorbent (Haroon et al. 2020; Nnadozie and Ajibade 2020). The slight increase was observed from 55 min; this could be explained by the longer agitation time in the sorption process (Khalil et al. 2021). After attaining the maximal adsorption capacity, equilibrium was attained, indicating that all the adsorbent's active sites were completely saturated with Cr (VI) and that the adsorbent had no more accessible functional groups to react the metal. These results are consistent with findings reported by Achary et al. (2020), Khalil et al. (2020), and Al et al. (2020).

Adsorption isotherm

To understand the Cr (VI) removal process in solution on the adsorbent *Sambucus nigra* L., it was necessary to analyze the equilibrium isotherm. The linear Langmuir equilibrium figure is presented in Fig. 5a, and the calculated parameters are summarized in Table 1. At 18 °C, the maximum adsorption

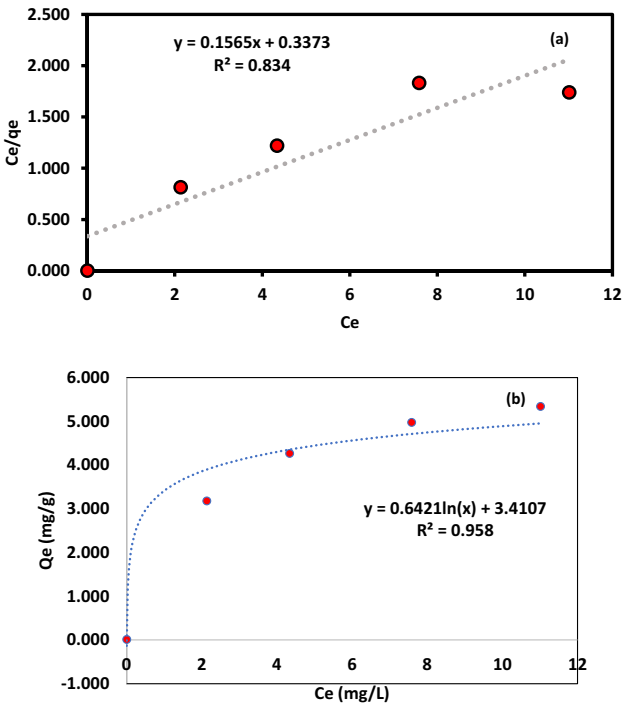

Fig. 5 Langmuir models for Cr (VI) adsorption: (**a**) Linear, (**b**) nonlinear regression

Table 1 Estimated constants for the linear Langmuir and Freundlich models

Isotherm models	Parameters	Values
Langmuir	q_m (mg/g)	6.389
	K_L (L/mg)	0.464
	R_L	0.301
	R^2	0.834
Freundlich	K_F (mg/g)	0.001
	N	0.175
	R^2	0.764

capacity (q_m) for complete coverage on the monolayer was 6.389 mg/g. This result shows that the nature of the adsorbent surface was homogeneous. Also, the R_L value is in the range of 0 to 1, which indicates that the adsorption process is favorable. These results agree with Nigam et al. (2019), Pathania et al. (2020), and Thabede et al. (2020).

The Freundlich isotherm is shown in Fig. 6a, and the equilibrium parameters are presented in Table 1. The value of 1/n comprised between 0 and 1 indicates a stronger binding to the adsorbent, i.e., a chemical process, whereas a value of 1/n more than 1.0 evidences an unfavorable removal process (Cherdchoo et al. 2019; Al et al. 2020). The result of 1/n = 5.72 being more than 1. Consequently, the adsorption process was not optimal with respect to the value of K_F = 0.001 mg/g, concluding that the laboratory analyses did not accommodate the linear form of Freundlich equation.

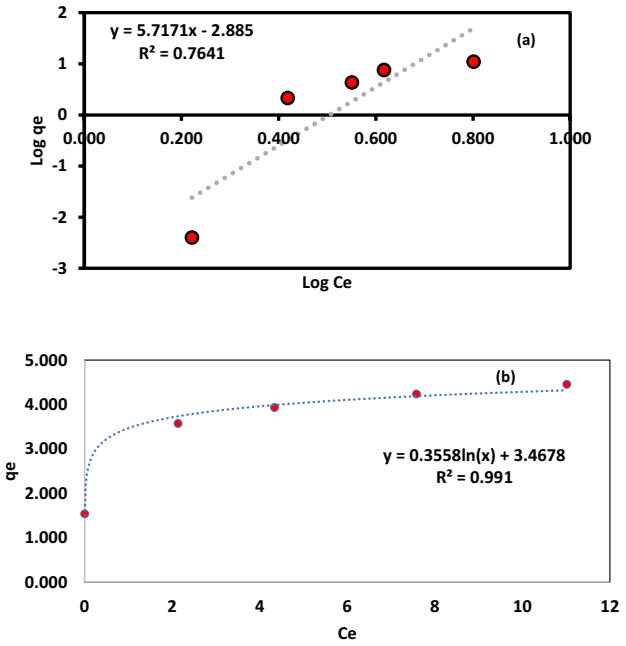

Fig. 6 Freundlich models for Cr (VI) adsorption: (**a**) Linear, (**b**) non-linear regression

The non-linear isotherms of Langmuir and Freundlich models are shown in Figs. 5b and 6b, respectively. The summarized data of non-linear models of Langmuir and Freundlich isotherms are shown in Table 2. The adsorption capacity of 1.557 (mg/g) can be attributed to a low initial solute concentration and a high adsorbent dosage which provides more adsorption active sites that even after the removal process remain unsaturated (Kumar and Chauhan 2019; Wang et al. 2020). In this regard, Cr (VI) ion forms a homogeneous monolayer with the active sites, so that when the adsorbent surface has formed a single layer, this can make the adsorption process not to continue forming adjacent layers (Neolaka et al. 2020). The non-linear models show that the R^2 values of adsorption process are 0.958 and 0.991 for Langmuir and Freundlich isotherms, repectively. These results are higher compared to linear model; hence, non-linear isotherm is better fit for the study.

Kinetic study

The modelling of heavy metal removal rate equations in liquid systems is to be analyzed using non-linear regression (Tan and Hameed 2017). The adsorption rate consists of three steps: the transfer of adsorbate to the adsorbent surface (film diffusion), the transfer of adsorbate from the surface to the active sites (intraparticle diffusion), and the binding of adsorbate to the active sites (Chandana et al. 2018). To determine the mechanisms involved in the sorption rate process, non-linear, pseudo-first order, pseudo-second order, and intra-particle diffusion kinetic models were analyzed, as shown in Table 3. To determine which of the models best fit the experimental data, the correlation value (R^2) closest to unity (1) was used. The pseudo-first order, pseudo-second order, and intra-particle diffusion values were compared, noting that the pseudo-second order (0.974) and intra-particle diffusion (0.928) equations showed higher correlation (R^2) values closer to unity. The good fit the pseudo-second order and intraparticle diffusion models which show that the removal of Cr (VI) ions was based on electrostatic interactions (Khalil et al. 2020). The models determined that

Table 2 Estimated constants for the non-linear Langmuir and Freundlich models

Isotherm models	Parameters	Values
Langmuir	q_m (mg/g)	1.557
	K_L (L/mg)	0.188
	R_L	0.301
	R^2	0.958
Freundlich	K_F (L/mg)	2936.3
	N	2.811
	R^2	0.991

Table 3 Calculated constants of the kinetic models for Cr (VI) adsorption on *Sambucus nigra* L. based on linear and non-linear models

Kinetic models	Parameters	Values
Linear model		
Pseudo-first order	K_1 (1/min)	0.003
	q_e (mg/g)	4.869
	R^2	0.848
Pseudo-second order	K_2 (g/mg min)	0.029
	q_e (mg/g)	2.412
	q_e (projected) (mg/g)	1.353
	R^2	0.996
Non-linear model		
Pseudo-first order	K_1 (1/min)	3.135
	q_e (mg/g)	4.650
	R^2	0.864
Pseudo-second order	K_2 (g/mg min)	2.847
	q_e (mg/g)	2.350
	q_e (projected) (mg/g)	1.353
	R^2	0.974
Intraparticle diffusion model	K_1 (1/min)	0.745
	R^2	0.928

adsorption occurred on the surface or through the pores of the adsorbent, characterizing it as chemical sorption or chemisorption.

Study of thermodynamic properties

Temperature variation affects the adsorption procedure by modifying the surface activity of the adsorbent along with the kinetic energy of the metal ions (Lima et al. 2019; Bazzazzadeh et al. 2020). The increase in Cr (VI) removal was observed by varying the temperature in the range 291–343 K. This effect conditioned the mobility of Cr (VI) ions and as well as the activity of the adsorbent functional groups (Shooto 2020a). The calculated values of the thermodynamic equilibrium parameters are presented in Table 4. Figure 7 shows that the sorption capacity of Cr (VI) increased as the solution temperature was higher. This effect demonstrates that high temperatures provide the metal ions with sufficient kinetic energy to overcome all the forces that hinder the removal processes (Shooto 2020a).

The positive value of ΔH° defines the endothermic condition in Cr (VI) removal. The result of entropy variation

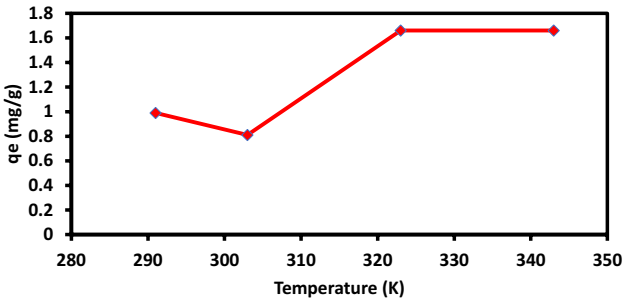

Fig. 7 Effect of Temperature on adsorption of Cr (VI) via *Sambucus nigra* L

ΔS° = 0.40 points to higher randomness at the solid–liquid interface, demonstrating higher sorption capacity of Cr (VI) ions (Mathai et al. 2022). It has been observed that the free energy changes (at temperatures of 303–343 K) are negative, while at 291 K, it is positive. Therefore, the adsorption of Cr (VI) at room temperature is not spontaneous, while at higher temperatures, it is spontaneous and feasible; these comparable results are reported by (Thabede et al. 2020; Al et al. 2020).

Comparative study

Adsorption is considered the most convenient, cost-effective, and user-friendly method for the removal of metal ions from an aqueous solution. Researchers have studied many adsorbents for the removal of pollutants from wastewater, such as agricultural wastes, forestry wastes, hydrogels, activated carbon, and nanoadsorbents (Mathai et al. 2022; Saha and Orvig 2010; Wang et al. 2020; Yadav et al. 2022; Yusuff et al. 2022). In this regard, the efficiency of metal ion removal depends on many factors, such as the composition of the adsorbents and the types of metals. This is one of the main reasons why adsorption studies have become one of the most active and frequent works of scientists.

Biosorbents with high adsorption capacity, low economic cost, high availability, less sludge generation, reusability, non-toxic, and environmentally friendly nature are characteristics that open a line of research to study new biomaterials specific to each region. In particular, biosorbents obtained from agricultural, animal and industrial waste are of great interest. However, the choice of a biosorbent for a given metal is not easy and requires many experiments and in-depth research (Singha et al.

Table 4 Thermodynamic analysis for Cr (VI)

ΔG° (KJ/mol)				ΔH° (KJ/mol K)	ΔS° (KJ/mol K)	Ea (KJ/mol)
Temperature K						
291	303	323	343			
0.52	− 4.29	− 12.31	− 20.33	117.21	0.40	− 105.92

2011). Forest residues such as elderberry leaves generated from industrial activity can be a promising material for adsorption research. This biomass is composed of dietary pigments; anthocyanins; flavonoids; lectins; lupeol; β-sitosterol; holocalin; prunasin; zierin; rutin; sambunigrin; tannin; choline; beltulin; vitamins A, B1, B2, B3, B5, B6, B9, C, and P; and minerals (Boroduske et al. 2021; Kalak et al. 2020). These substances contain polar functional groups, such as carboxyl, phenolic, hydroxyl, sulpho, and amino groups that are able to bind metal ions. The binding mechanism may involve reactions such as electrostatic interactions, complexation, microprecipitation, and chelation (Khalil et al. 2021; Saha and Orvig 2010). Table 5 shows the comparative data of the results achieved by the leaves of *Sambucus nigra* L. in the treatment of wastewater having Cr (VI) with other biomasses reported in the literature. The comparison revealed that the adsorbent generated by the leaves of *Sambucus nigra* L., as leftover biomass from agroforestry and industrial activity, is a low-cost adsorbent with superior performance in the removal at low concentrations and without chemical activation. Consequently, it is worthwhile to study the removal capacity of Cr(VI) ions with native forest residues. The *Sambucus nigra* L. (elderberry) tree grows rapidly and is widely available in many regions of Peru, producing large quantities of leaves and bark that are discarded as solid waste.

Elderberry leaves have never been explored as a adsorbent for Cr(VI) removal in Peru, and this is the first study which show the adsorption capacity of native *Sambucus nigra* L. These results demonstrate the significance of this biomass in industrial effluent remediation applications.

Adsorption mechanism of Cr(VI) via FTIR spectrum

The characterization of Cr(VI) adsorption mechanisms through *Sambucus nigra* L. (SNL) leaves using Fourier transform infrared (FTIR) spectra is presented in Fig. 8. The spectrum of Cr(VI) before and after adsorption was examined between 4000 and 400 cm^{-1} wavenumbers, which is shown in the figure as SNL and SNLCr(VI) for before and after adsorption, respectively. The peaks at 2921 and 2851 cm^{-1} correspond to alkane C-H stretching, whereas the peaks at 1730 and 1713 cm^{-1} indicate C = O stretching (carbonyl group), as shown by both spectra SNL and SNLCr (VI) (Moldovan et al. 2016). The band 1651 cm^{-1} corresponds to C = C vibrations, while the band 1683 to 1685 cm^{-1} for SNL to SNLCr(VI) spectra shows a minor shift. After Cr adsorption, the spectrum exhibits peaks at 1643, 1632, 1623, 1614, 1577, 1572, 1567, 1540, 1530, 1508, 1498, 1488, 1427, 1386, 1269, 806, 757, 520, and 464 cm^{-1} which are absent from SNL spectra. The FTIR spectra range from 4000 to 400 cm^{-1} is shown in Fig. 8I, and two range graphs are shown in Fig. 8II and III to better comprehend the peaks changes before and after adsorption. Spectrum peaks on the surface of SNLCr(VI) obtained at 1643, 1632, 1623, and 1614 cm^{-1} (in Fig. 8 zone a) are ascribed to the C = C stretching, indicating the presence of alkene groups. Chromium may attach to unsaturated alkene molecules. Peak 1594 cm^{-1} is not present in

Table 5 Comparison of Cr (VI) adsorption capacity with other adsorbents

Adsorbent	Maximum capacity (mg/g)	Dose g/L	T° C	pH	Best fitting isotherm and kinetics	References
Coffee and tea residue	87.72 94.34	2	30	2	Freundlich and pseudo-second order	(Cherdchoo et al. 2019)
Tea residues	79.08	6	30	3.9	Langmuir and pseudo-second order	(Nigam et al. 2019)
Black cumin seeds	9.98	1	40	1	Langmuir and pseudo-second order	(Thabede et al. 2020)
Harpagophytum residues	77.24	0.19	35	1	Freundlich and pseudo-second order	(Shooto 2020b)
Hyacinth and Lemnaminor Leaves	79.24 61.0	1 1	25 ± 1 25 ± 1	2 2	Langmuir and pseudo-second order; Langmuir and pseudo-second order	(Balasubramanian et al. 2020)
Mango bark	78.96	0.12	30	2	Langmuir and pseudo-second order	(Pathania et al. 2020)
Mentha piperita	29.23	0.45	25	2	Freundlich and pseudo-second order	(Al et al. 2020)
Acacia sawdust	6.34	4.9	30	2	Langmuir and pseudo-second order	(Khalil et al. 2020)
Rice husk	379.63	0.6	20 ± 2	5.2	Langmuir and pseudo-second order	(Khalil et al. 2021)
Hyacinth root	1.28	14	25 ± 5	3	Freundlich and pseudo second order	(Kumar & Chauhan 2019)
Acorus calamus	14.64	0.2	25	1	Langmuir and pseudo-second order	(Shooto 2020a)
Sambucus nigra L	6.39	3	18	2	Non-linear Freundlich, pseudo-second order, and intra-particle diffusion	Present study

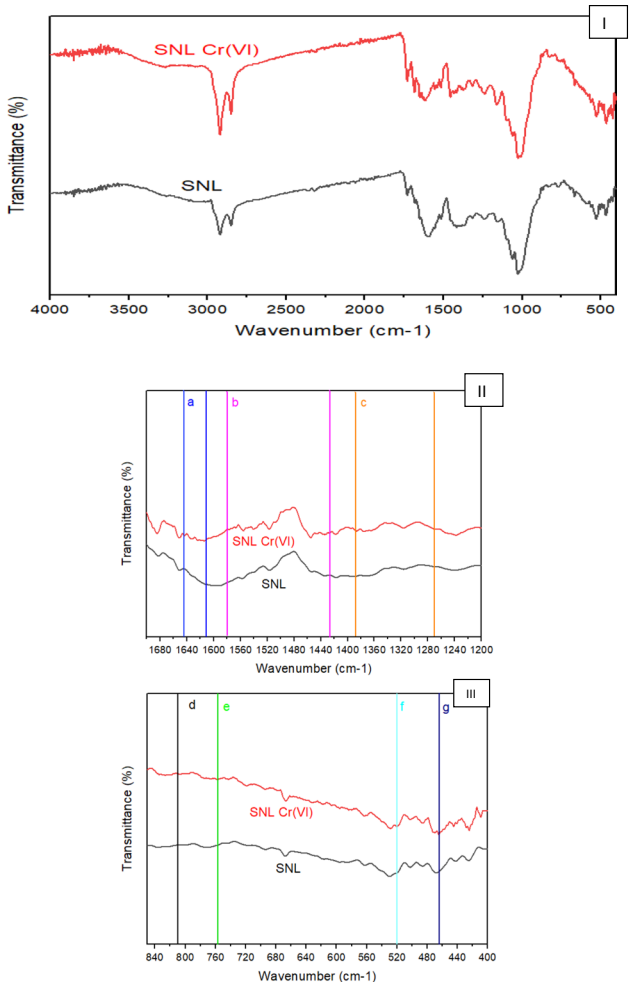

Fig. 8 FTIR spectrum graph of SNL and SNL Cr(VI) (before and after adsorption process). (I), Complete spectra range from 4000 to 400 cm^{-1}. (II), Spectra range from 1700 to 1200 cm^{-1}. (III), Spectra range from 860 to 400 $cm.^{-1}$

SNLCr(VI); however, a few additional peaks (1577, 1572, 1567, 1540, 1530, 1508, 1498, 1488, and 1427 cm^{-1}) (in Fig. 8 zone b) exist, indicating peak displacement owing to chromium loading on the surface of SNL. These peaks correspond to the N–H bend of amine with an unsaturated hydrocarbon functional group. The existence of chromium in the form of $(NH_4)_2Cr_2O_7$ is strongly supported by the N–H bending vibrations at these peak ranges (Schutte and Heyns 1970; Monico et al. 2016). Peaks 806 and 757 cm^{-1} are in the chromate (CrO_4^{2-}) region, which are the source of asymmetric bridge (Cr–O–Cr) vibrations in $Cr_2O_7^{2-}$ and Cr–O stretching vibrations (Thangagiri et al. 2022). The peaks at 1386 and 1269 cm^{-1} (in Fig. 8 zone c) are caused by C-H bending and C-O stretching, indicating the presence of alcohol, carboxylic acid, or phenols (Shahadat et al. 2015). Peak at 585 $cm-^{1}$, which corresponds to alkyl halides, is present in SNL but not in SNLCr(VI), due to peak shifting, and additional lower frequency peaks are present in SNLCr (VI). The vibrational of O–Cr–O or Cl–Cr–Cl is seen at lower frequencies (520, 464, and 409 cm^{-1}) (Sopotrajanov et al. 1999).

Other peaks are practically the same in both compounds SNL and SNLCr(VI) precise few which are slightly (1–10 cm^{-1}) shifted that are also due to chromium loading (Singha et al. 2011). The FTIR analysis indicates chromium loading on compounds during the adsorption process.

XRD analysis

The chromium adsorption phenomenon by *Sambucus nigra* L. was also studied using XRD. The XRD pattern of the produced *Sambucus nigra* L. (SNL) is shown in Fig. 9, revealing the biomaterial's amorphous nature. However, the few prominent peaks seen in the XRD at 24.34° and 31.15° can be attributed to the carbon diffraction planes in the biomaterial (Chellappan et al. 2018). X'Pert HighScore software was used for the analysis. The results established the presence of polyphenolic compounds in the SNL. Peak matches the reference number 01–076-1367, indicating the presence of potassium compounds with hydrocarbon groups.

The XRD pattern of the utilized SNL for the chromium adsorption is shown in Fig. 10. The halo of

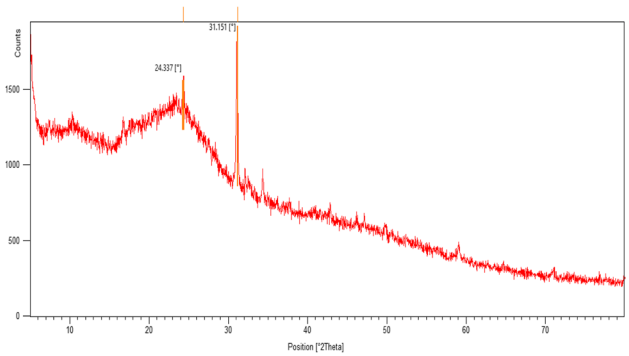

Fig. 9 XRD of SNL (before adsorption)

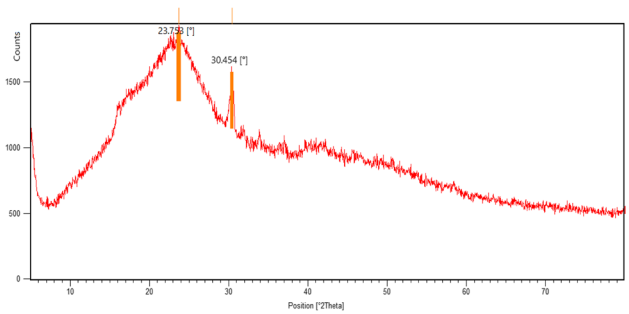

Fig. 10 XRD of Cr-SNL (after adsorption)

diffraction at 23.75°and sharp peak at 30.45° are the indicative of presence of chromium ions on the plant biomaterial (Thangagiri et al. 2022). The results indicated that chromium adsorption on this biomaterial is achievable, which was validated by XRD data. The XRD analysis also supports the presence of ammonium chromium oxide as mentioned in the FTIR analysis section. The peak seen in Cr-SNL corresponds to the reference code 01–075-1578. Two other reference card codes 01–084-1201 and 00–028-1188, coincide with the identified XRD peaks of the Cr-SNL sample, indicating the potential of chromium phosphate and sodium chromium phosphate compounds. Furthermore, the XRD pattern of the used biomaterial is observed the same as those of fresh material (Figs. 9 and 10) representing that there is no change in the amorphous structure of biomaterial being used (Gu et al. 2022).

SEM and EDS analysis

The SEM image of the utilized *Sambucus nigra* L. in the chromium removal is shown in Fig. 11, which confirmed the amorphous structure of the biomaterial, already revealed in XRD. The adsorbed chromium is accumulated the *Sambucus nigra* L. biomaterial and it is shown in the figure at the spectrum 17 as white spots. The EDS of spectrum 17 confirms the presence of chromium ions on the biomaterial and patches of white pattern on the SEM image are the evidence of the presence of the adsorbed chromium ions. Similar observation was reported earlier by Amaku et al.

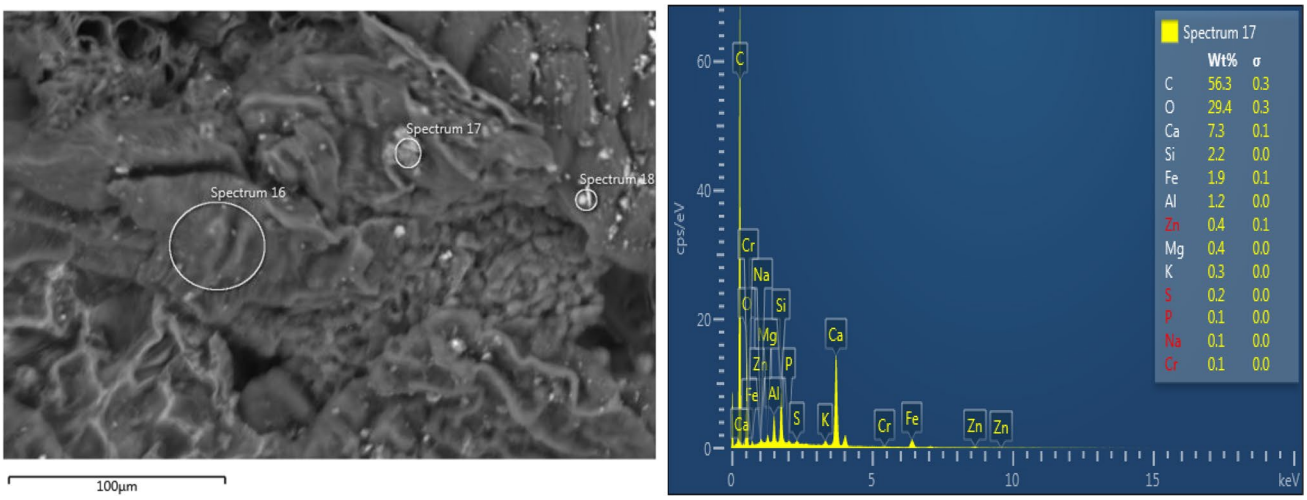

Fig. 11 SEM and EDS spectrum of Cr-SNL (spectrum-17)

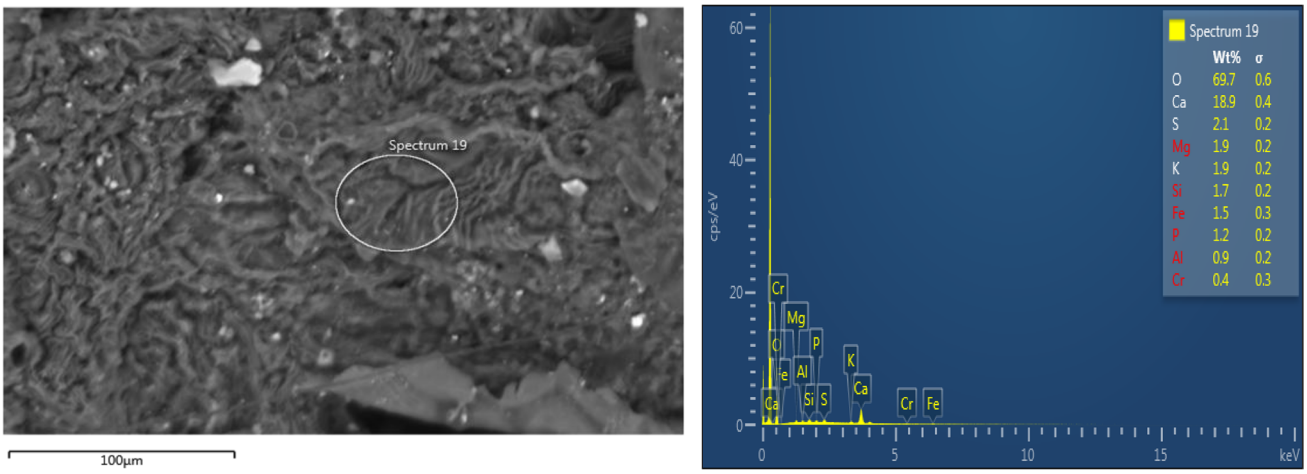

Fig. 12 SEM and EDS spectrum of Cr-SNL (spectrum-19)

(2021) for the chromium removal using extract of *Dacryodes edulis* leaves.

The another SEM image of the utilized SNL is presented in the Fig. 12, which is also confirmed by the presence of adsorbed chromium in the material and it is confirmed in the EDS of spectrum 19. In addition to chromium ions, silicon, iron, and aluminum ions are observed.

ICP-OES analysis

Furthermore, chromium adsorption was validated using the ICP-OES. ICP-OES equipment was used to evaluate the SNL and SNL-Cr samples. The acquired findings clearly demonstrated the chromium adsorption via *Sambucus nigra* L. Before adsorption, ICP-OES measurement revealed a chromium value of < 0.0003 µg/L, but after batch adsorption, the result was 1720.37 µg/L.

Conclusion

This study describes the utilization of agroforestry and industrial residue *Sambucus nigra* L. as a novel physical adsorbent for the removal of Cr (VI), as an environmentally friendly and low-cost solution. The adsorption process experimental results best fitted the non-linear Freundlich equilibrium model. The sorption of Cr (VI) onto the adsorbent was rapid, reaching equilibrium and stabilizing within 35 min. The pseudo-second-order model defining the phenomena with a chemical ion exchange mechanism best depicted the elimination process. The thermodynamic parameters revealed that the occurrence was both spontaneous and favorable. The result of adsorption is strongly supported by XRD, FTIR, SEM–EDS, and ICP-OES analyses. The results of these analyses provide significant evidence for chromium adsorption via *Sambucus nigra* L. As a conclusion, it has been demonstrated that this novel adsorbent can be useful to manage chromium in industrial wastewater.

Acknowledgements The authors are grateful to the editor and reviewers for improving the quality of the manuscript.

Author contribution All authors contributed to the study conception and design. Material preparation and data collection were performed by HBM, MRC, PCA, JPP, and CTT, and analysis part contributed by MKJ and GG. The first draft of the manuscript was written by HBM, and all authors commented on previous versions of the manuscript and modified. All authors read and approved the final manuscript.

Funding This work was supported by the National University of Central Peru, Research Institute of the Faculty of Agronomy, to carry out the adsorption study of low-cost biomass leaves (*Sambucus Nigra* L.) in the removal of Cr(VI) ions in an aqueous solution.

Data availability Not applicable.

Declarations

Ethics approval and consent to participate Not applicable.

Consent for publication Not applicable.

Conflict of interest The authors declare no competing interests.

References

Achary G, Ghosh M, Mishra S (2020) Insights into the modeling and application of some low cost adsorbents towards Cr(VI) adsorption. Mater Today: Proceedings 30:267–273. https://doi.org/10.1016/j.matpr.2020.01.433

Ağalar H (2019) Elderberry (Sambucus nigra L.). In Nonvitamin and Nonmineral Nutritional Supplements 3.14:211–215. https://doi.org/10.1016/B978-0-12-812491-8.00030-8

Al S, Tanweer M, Alam M (2020) Kinetic, isothermal, thermodynamic and adsorption studies on Mentha piperita using ICP-OES. Surf Interfaces 19:1–33. https://doi.org/10.1016/j.surfin.2020.100516

Amaku James F, Ogundare S, Akpomie Kovo G, Ibeji Collins U, Conradie J (2021) Functionalized MWCNTs-quartzite nanocomposite coated with Dacryodes edulis stem bark extract for the attenuation of hexavalent chromium. Sci Rep 11(1):12684. https://doi.org/10.1038/s41598-021-92266-0

Balasubramanian U, Murugaiyan S, Marimuthu T (2020) Enhanced adsorption of Cr(VI), Ni(II) ions from aqueous solution using modified Eichhornia crassipes and Lemna minor. Environ Sci Pollut Res 27:20648–20662. https://doi.org/10.1007/s11356-019-06357-7

Baruffi P, Olave de Freitas V, Machry K, Costa AR, Silveira G (2019) Evaluation of the potential of coal fly ash produced by gasification as hexavalent chromium adsorbent. Environ Sci Pollut Res 26:28603–28613. https://doi.org/10.1007/s11356-018-3852-7

Bazzazzadeh R, Soudi M, Valinassab T, Moradlou O (2020) Kinetics and equilibrium studies on biosorption of hexavalent chromium from leather tanning wastewater by Sargassum tenerrimum from Chabahar-Bay Iran. Algal Res 48:1–11. https://doi.org/10.1016/j.algal.2020.101896

Beksissa R, Tekola B, Ayala T, Dame B (2021) Investigation of the adsorption performance of acid treated lignite coal for Cr (VI) removal from aqueous solution. Environ Challenges 4:1–10. https://doi.org/10.1016/j.envc.2021.100091

Boroduske A, Jekabsons K, Riekstina U, Muceniece R, Rostoks N, Nakurte I (2021) Wild Sambucus nigra L. from north-east edge of the species range: a valuable germplasm with inhibitory capacity against SARS-CoV2 S-protein RBD and hACE2 binding in vitro. Ind Crops Prod 165(0). https://doi.org/10.1016/j.indcrop.2021.113438

Chandana L, Krushnamurty K, Suryakala D, Subrahmanyam C (2018) Low-cost adsorbent derived from the coconut shell for the removal of hexavalent chromium from aqueous medium. Mater Today: Proceedings 26:44–51. https://doi.org/10.1016/j.matpr.2019.04.205

Chellappan S, Nair V, Sajith V, Aparna K (2018) Synthesis, optimization and characterization of biochar based catalyst from sawdust for simultaneous esterification and transesterification. Chin J Chem Eng 26:2654–2663. https://doi.org/10.1016/j.cjche.2018.02.034

Cherdchoo W, Nithettham S, Charoenpanich J (2019) Removal of Cr(VI) from synthetic wastewater by adsorption onto coffee ground and mixed waste tea. Chemosphere 221:758–767. https://doi.org/10.1016/j.chemosphere.2019.01.100

Domínguez R, Zhang L, Rocchetti G, Lucini L, Pateiro M, Munekata PES, Lorenzo JM (2020) Elderberry (Sambucus nigra L.) as potential source of antioxidants. Characterization, optimization

of extraction parameters and bioactive properties. Food Chem 330(0). https://doi.org/10.1016/j.foodchem.2020.127266
Filip G, Florea A, Olteanu D, Clichici S, David L, Moldovan B, Cenariu M, Scrobota I, Potara M, Baldea I (2021) Biosynthesis of silver nanoparticles using Sambucus nigra L. fruit extract for targeting cell death in oral dysplastic cells. Mater Sci Eng C 123(0) https://doi.org/10.1016/j.msec.2021.111974
Freundlich H (1906) Adsorption in solution. Phys Chem Soc 40:1361–1368
Ghorbani F, Kamari S, Zamani S, Akbari S, Salehi M (2020) Optimization and modeling of aqueous Cr(VI) adsorption onto activated carbon prepared from sugar beet bagasse agricultural waste by application of response surface methodology. Surf Interfaces 18:1–12. https://doi.org/10.1016/j.surfin.2020.100444
Gu J, Dong Y, Zhang J (2022) Comparative study of four different flavonoid compounds-containing plant extracts functionalised waste wool for accelerating aqueous chromium(VI) reductive removal. Color Technol 138:97–113. https://doi.org/10.1111/cote.12575
Haroon H, Shah J, Khan M, Alam T, Khan R, Asad S, Ali M, Farooq G, Iqbal M, Bilal M (2020) Activated carbon from a specific plant precursor biomass for hazardous Cr(VI) adsorption and recovery studies in batch and column reactors: isotherm and kinetic modeling. J Water Process Eng 38:1–15. https://doi.org/10.1016/j.jwpe.2020.101577
Huaccho J, Balladares A, Yanac W, Rodríguez L, Villar M (2020) Review of antiviral and immunomodulatory effects of herbal medicine with reference to pandemic COVID-19. Archivos Venezolanos De Farmacologia y Terapeutica 39:795–807. https://doi.org/10.5281/zenodo.4407706
Ighalo J, Adeniyi A (2020) Adsorption of pollutants by plant bark derived adsorbents: an empirical review. J Water Process Eng 35:1–24. https://doi.org/10.1016/j.jwpe.2020.101228
Instituto Nacional De Defensa De La Competencia Y De La Proteccion De La Propiedad Intelectual (2018) Sauco. Retrieved from https://indecopi.gob.pe/documents/3015875/3019093/Bolet%C3%ADn+N%C2%B0+1+-+Sauco/dd154068-3526-7126-4eaa-f0b7cab87eb7. Accessed 8 February 2022
Kalak T, Dudczak J, Tachibana Y, Cierpiszewski R (2020) Effective use of elderberry (Sambucus nigra) pomace in biosorption processes of Fe(III) ions. Chemosphere 246:1–8. https://doi.org/10.1016/j.chemosphere.2019.125744
Khalid R, Aslam Z, Abbas A, Ahmad W, Ramzan N, Shawabkeh R (2018) Adsorptive potential of Acacia nilotica based adsorbent for chromium(VI) from an aqueous phase. Chin J Chem Eng 26:614–622. https://doi.org/10.1016/j.cjche.2017.08.017
Khalil U, Bilal M, Ali S, Rizwan M, Nasser M, Wijaya L (2020) Adsorption-reduction performance of tea waste and rice husk biochars for Cr(VI) elimination from wastewater. J Saudi Chem Soc 24:799–810. https://doi.org/10.1016/j.jscs.2020.07.001
Khalil U, Shakoor M, Ali S, Ahmad S, Rizwan M, Alsahli A, Alyemeni M (2021) Selective removal of hexavalent chromium from wastewater by rice husk: kinetic, isotherm and spectroscopic investigation. Water 13:1–12. https://doi.org/10.3390/w13030263
Kumar P, Chauhan M (2019) Adsorption of chromium (VI) from the synthetic aqueous solution using chemically modified dried water hyacinth roots. J Environ Chem Eng 7:1–8. https://doi.org/10.1016/j.jece.2019.103218
Labied R, Benturki O, Eddine AY, Donnot A (2018) Adsorption of hexavalent chromium by activated carbon obtained from a waste lignocellulosic material (Ziziphus jujuba cores): kinetic, equilibrium, and thermodynamic study. Adsorpt Sci Technol 36:1066–1099. https://doi.org/10.1177/0263617417750739
Langmuir I (1918) The adsorption of gases on plane surfaces of glass, mica, and platinum. J Am Chem Soc 40:1361–1368. https://pubs.acs.org/doi/pdf/10.1021/ja02242a004
Lavado-Meza C, Asencios YJO, Cisneros-Santos G, Unchupaico-Payano I (2021) Removal of methylene blue dye using Nostoc commune biomass: kinetic, equilibrium and thermodynamic study. Revista Mexicana de Ingeniería Química 20:941–954. https://doi.org/10.24275/rmiq/IA2291
Lima EC, Bandegharaei AH, Piraján JCM, Anastopoulos I (2019) A critical review of the estimation of the thermodynamic parameters on adsorption equilibria. Wrong use of equilibrium constant in the Van't Hoof equation for calculation of thermodynamic parameters of adsorption. J Mol Liq 273:425–434. https://doi.org/10.1016/j.molliq.2018.10.048
Mathai R, Chatterjee J, Kumar S, Kumar M (2022) Adsorption of chromium (VI) from aqueous phase using Aegle marmelos leaves: kinetics, isotherm and thermodynamic studies. Chem Data Collect 39:100871. https://doi.org/10.1016/j.cdc.2022.100871
Moldovan B, David L, Achim M, Clichici S, Filip G (2016) A green approach to phytomediated synthesis of silver nanoparticles using Sambucus nigra L. fruits extract and their antioxidant activity. J Mol Liq 221(0):271–278. https://doi.org/10.1016/j.molliq.2016.06.003
Monico L, Janssens K, Cotte M, Sorace L, Vanmeert F, Brunetti B, Miliani C (2016) Chromium speciation methods and infrared spectroscopy for studying the chemical reactivity of lead chromate-based pigments in oil medium. Microchem J 124:272–282. https://doi.org/10.1016/j.microc.2015.08.028
Mughal N, Arif A, Jain V, Chupradit S, Shabbir MS, Ramos C, Zhanbayev R (2022) The role of technological innovation in environmental pollution, energy consumption and sustainable economic growth: evidence from South Asian economies. Energ Strat Rev 39:1–6. https://doi.org/10.1016/j.esr.2021.100745
Navas A, Hernández J, Velásquez J (2021) Production and quality of forage of Sambucus nigra in living fences, high Colombian tropics. Agron Mesoam 32(0):523–537. https://doi.org/10.15517/am.v32i2.42862
Neolaka Y, Lawa Y, Naat J, Riwu A, Iqbal M, Darmokoesoemo H, Kusuma H (2020) The adsorption of Cr(VI) from water samples using graphene oxide-magnetic (GO-Fe3O4) synthesized from natural cellulose-based graphite (kusambi wood or Schleichera oleosa): Study of kinetics, isotherms and thermodynamics. J Market Res 9:6544–6556. https://doi.org/10.1016/j.jmrt.2020.04.040
Nigam M, Rajoriya S, Rani S, Kumar P (2019) Adsorption of Cr (VI) ion from tannery wastewater on tea waste: kinetics, equilibrium and thermodynamics studies. J Environ Chem Eng 7:1–9. https://doi.org/10.1016/j.jece.2019.103188
Nnadozie E, Ajibade P (2020) Adsorption, kinetic and mechanistic studies of Pb(II) and Cr(VI) ions using APTES functionalized magnetic biochar. Microporous Mesoporous Mater 309:1–9. https://doi.org/10.1016/j.micromeso.2020.110573
Pathania D, Sharma A, Srivastava A (2020) Modelling studies for remediation of Cr (VI) from wastewater by activated Mangifera indica bark. Curr Res Green Sustain Chem 3:1–34. https://doi.org/10.1016/j.crgsc.2020.100034
Peng X, Tang P, Yang S, Fu S (2020) How should mining firms invest in the multidimensions of corporate social responsibility? Evidence from China. Resour Policy 65:1–14. https://doi.org/10.1016/j.resourpol.2019.101576
Quiñones J, Cardona J, Castro E (2020) Fodder shrub silage for livestock feeding systems in the high Andean tropics. Rev Investig Altoandin 22(0):3–285. https://doi.org/10.18271/ria.2020.662
Ray S, Gusain R, Kumar N (2020) Adsorption in the context of water purification. In Carbon Nanomaterial-Based Adsorbents for Water Purification. Elsevier, pp. 67–100 https://doi.org/10.1016/b978-0-12-821959-1.00004-0
Rouhaninezhad A, Hojati S, Masir M (2020) Adsorption of Cr (VI) onto micro and nanoparticles of palygorskite in aqueous solutions: effects of pH and humic acid. Ecotoxicol Environ Saf 206:1–8. https://doi.org/10.1016/j.ecoenv.2020.111247

Ruíz M, Mejía F (2020) Plants used in traditional medicine for viral respiratory conditions. REBIOL 40(0):109–130. https://doi.org/10.17268/rebiol.2020.40.01.12

Saha B, Orvig C (2010) Biosorbents for hexavalent chromium elimination from industrial and municipal effluents. Coord Chem Rev 254:2959–2972. https://doi.org/10.1016/j.ccr.2010.06.005

Schutte C, Heyns A (1970) Low-temperature infrared studies Vi. the Infrared Spectra of Ammonium Dichromate and Ammonium Dichromate. J Mol Struct 5(0):37–48

Shahadat M, Rafatullah M, Teng TT (2015) Characterization and sorption behavior of natural adsorbent for exclusion of chromium ions from industrial effluents. Desalin Water Treat 53:1395–1403. https://doi.org/10.1080/19443994.2013.855678

Shen T, Ke AL (1986) The distribution of chromium(VI) species in solution as a function of pH and concentration. Talanta 33(9):775–777. https://doi.org/10.1016/0039-9140(86)80187-4

Shooto N (2020a) Removal of toxic hexavalent chromium (Cr(VI)) and divalent lead (Pb(II)) ions from aqueous solution by modified rhizomes of Acorus calamus. Surf Interfaces 20:1–9. https://doi.org/10.1016/j.surfin.2020.100624

Shooto N (2020b) Removal of lead(II) and chromium(VI) ions from synthetic wastewater by the roots of harpagophytum procumbens plant. J Environ Chem Eng 8:1–12. https://doi.org/10.1016/j.jece.2020.104541

Singha B, Kumar T, Kumar A, Das S (2011) Cr(VI) Ions removal from aqueous solutions using natural adsorbents – FTIR studies. J Environ Prot 02:729–735. https://doi.org/10.4236/jep.2011.26084

Sopotrajanov B, Stefov V, Minjas Z, Petruševski V (1999) Fourier transform infrared and Raman spectra of the green chromium(III) chloride hexahydrate. J Mol Struct 482:109–113

Spessato L, Duarte VA, Viero P, Zanella H, Fonseca JM, Arroyo PA, Almeida VC (2021) Optimization of sibipiruna activated carbon preparation by simplex-centroid mixture design for simultaneous adsorption of rhodamine B and metformin. J Hazard Mater 411:125166. https://doi.org/10.1016/j.jhazmat.2021.125166

Tan KL, Hameed BH (2017) Insight into the adsorption kinetics models for the removal of contaminants from aqueous solutions. J Taiwan Inst Chem Eng 74:25–48. https://doi.org/10.1016/j.jtice.2017.01.024

Tao F, Wang Y, Zhao Z, Liu X, Zhang G, Li C, Wang Z, Huo Q (2021) Effective removal of Cr(VI) in aqueous solutions using Caulis lonicerae residue fermented by Phanerochaete chrysosporium. Prep Biochem Biotechnol 51:842–851. https://doi.org/10.1080/10826068.2020.1805623

Tejada C, Villabona A, Ortega R, Bonilla H, Espinoza F (2021) Potential use of residual sawdust of Eucalyptus Globulus Labill in Pb (II) adsorption: Modelling of the kinetics and equilibrium. Appl Sci (Switzerland) 11(0). https://doi.org/10.3390/app11073125

Thabede P, Shooto N, Xaba T, Naidoo E (2020) Adsorption studies of toxic cadmium(II) and chromium(VI) ions from aqueous solution by activated black cumin (Nigella sativa) seeds. J Environ Chem Eng 8:1–12. https://doi.org/10.1016/j.jece.2020.104045

Thangagiri B, Sakthivel A, Jeyasubramanian K, Seenivasan S, Dhaveethu RJ, Yun K (2022) Removal of hexavalent chromium by biochar derived from Azadirachta indica leaves: batch and column studies. Chemosphere 286:1–16. https://doi.org/10.1016/j.chemosphere.2021.131598

US EPA (2022) Basic information about chromium in drinking water. Retrieved June 21 2022, from https://www.epa.gov/ground-water-and-drinking-water/national-primary-drinking-water-regulations

Wang Q, Zhou C, Kuang YJ, Jiang ZH, Yang M (2020) Removal of hexavalent chromium in aquatic solutions by pomelo peel. Water Sci Eng 13:65–73. https://doi.org/10.1016/j.wse.2019.12.011

WHO (n.d.) report History of Guideline Development, Chromium. Retrieved June, 2022, from https://cdn.who.int/media/docs/default-source/wash-documents/wash-chemicals/chromium_history.pdf?sfvrsn=971a14cb_3

WHO (2020) Chromium in drinking-water. In: Background document for development ofWHO Guidelines for drinking-water quality. World Health Organization (WHO/HEP/ECH/WSH/2020.3), Geneva. Retrieved from https://apps.who.int/iris/bitstream/handle/10665/338062/WHO-HEP-ECH-WSH-2020.3-eng.pdf?sequence=1&isAllowed=y

Yadav M, Thakore S, Jadeja R (2022) Removal of organic dyes using Fucus vesiculosus seaweed bioadsorbent an ecofriendly approach: equilibrium, kinetics and thermodynamic studies. Environ Chem Ecotoxicol 4:67–77. https://doi.org/10.1016/j.enceco.2021.12.003

Yusuff A, Lala M, Thompson K, Babatunde E (2022) ZnCl2-modified eucalyptus bark biochar as adsorbent: preparation, characterization and its application in adsorption of Cr(VI) from aqueous solutions. S Afr J Chem Eng 42:138–145. https://doi.org/10.1016/j.sajce.2022.08.002